A new multisine-based impedimetric aptasensing platform

A new multisine-based impedimetric aptasening platform

Danny Pauwels[a], Sanaz Pilehvar[b], Bart Geboes[a], Annick Hubin[c], Karolien De Wael[b], Tom Breugelmans[a,c]*

[a]*University of Antwerp, Research Group Advanced Reactor Technology, Universiteitsplein 1, 2610 Wilrijk, Belgium.*
[b]*University of Antwerp, Research Group Antwerp X-ray analysis, Electrochemistry and Speciation, Groenenborgerlaan 171, 2020 Antwerp, Belgium.*
[c]*Vrije Universiteit Brussel, Research Group Electrochemical and Surface Engineering, Pleinlaan 2, 1050 Brussels, Belgium*
**Corresponding Author: tom.breugelmans@uantwerpen.be*

Abstract

In this work an aptamer-based biosensor is combined with a multisine electrochemical impedance spectroscopy sensing methodology into a novel and promising biosensing strategy. Employing a multisine instead of a traditional single sine measuring method allows the detection and quantification of parameters that provide information about the accuracy and reliability of the results, such as noise and distortions. This does not only lead to a shorter measurement time, but it also enables an easy and fast evaluation of the quality of the data and fitting, leading to more accurate results.

Keywords: multisine impedance spectroscopy, aptamer, biosensor

1. Introduction

An electrochemical aptamer-based biosensor employs aptamers as a biochemical recognition element in combination with an electrochemical technique as the transducer to convert the detection into a measurable signal. Aptamers are single-stranded nucleic acids that selectively bind to target molecules. Biosensors offer a promising alternative to traditional chromatographic techniques (often coupled with mass spectrometry) such as GC [1–4] or LC [5–8], which often are used to detect and quantify hazardous materials. These techniques are well-known and widely-used, but they are often attributed a number of disadvantages, such as the requirement of sophisticated and expensive equipment, which requires trained personnel to operate and the often complex and time-consuming sample preparation [9–12]. Electrochemical biosensors can reach the same level of sensitivity and accuracy while offering several other advantages such as low cost, fast screening, simple operation and the possibility for in-situ screening and offer a promising sensing strategy [13–18]. The electrochemical method employed plays a significant role in the performance of the sensor. Although amperometric techniques [18,19] have shown an improvement over earlier published non-electrochemical determination methods [20], it is believed that electrochemical impedance spectroscopy (EIS) is more favorable than other electrochemical detection techniques since significantly large differences in low target concentration range are usually obtained due to the inverse relation of the impedance with the current [13,21,22].

When EIS is used, the results are interpreted by fitting a model to the data and extracting the values of the corresponding electrical components. To obtain a satisfactory model for an electrochemical system, the system needs to fulfil the conditions of causality, linearity and stationarity [23]. To check whether these conditions are fulfilled, different methods are described in literature. Possibly the best known are the Kramers-

Kronig relations [24,25] and the Z-HIT procedure (Hilbert Transform) [26,27]. It is known that electrochemical systems can have strong non-linear behaviour and the detection of non-linear and non-stationary behaviour is therefore of great importance, especially in the application of a biosensor for hazardous contaminants where accuracy and reliability of the results is very important. However, this is often forgotten and to overcome this problem, we employ an integrated methodology to measure, analyse and model electrochemical systems in a correct and reliable way. This methodology is a multisine EIS procedure based on an odd random phase multisine excitation signal (ORP-EIS). Multisine is a term for broadband EIS where the excitation signal that is applied, consists of the sum of multiple sine signals. The methodology employed in this work was developed in the Research Group Electrochemical and Surface Engineering (SURF) from the Vrije Universiteit Brussel. The theoretical background of the methodology is described in [28,29]. The advantages and application of the methodology are demonstrated in [30–32]. This technique allows to measure and quantify the level of disturbing noise, the level of the non-linear distortions and the level of the non-stationary behaviour, enabling the researcher to evaluate if the measurement conditions are met. These results are then taken into account in the modelling and fitting of the data, resulting in a more accurate value for the impedance. In addition, the application of a broadband multisine signal also decreases measurement time considerably [30].

It is clear that the advantages of a multisine signal over a single sine signal, when applied to an impedimetric biosensor, lead to a faster, more accurate and more reliable sensing device. However, to the best of our knowledge, impedimetric biosensors are currently always measured with single sine EIS. No reports were found in literature of a multisine imepdimetric biosensing platform. In this work, the feasibility of employing a multisine signal for an impedimetric biosensor is studied. A comparison to single sine EIS is made to validate the technique while the additional information is used to assess the measurements as well as the model that is used for the fitting procedure. As a case study, measurements are performed on a hydroxylated PCB (OH-PCB), which exhibits significant toxic health effects to humans and wildlife [20,33–38] and has a distinct presence in the environment [9].

2. Experimental

2.1. Chemicals and Equipment

$K_3[Fe(CN)_6]$ (p.a., ≥99 %), $K_4[Fe(CN)_6]$ (p.a., ≥99 %), N-(3-Dimethylaminopropyl)-N′-ethylcarbodiimide hydrochloride (EDC) (BioXtra, ≥99,9 %), N-hydroxysuccinimide (NHS) (98 %) and multi-walled carbon nanotubes (MWCNTs, i.d. = 2-15 nm, length = 1-10 µm) were purchased from Sigma-Aldrich. 2-hydroxy-2',3',4',5,5'-pentachlorobiphenyl (OH-PCB) was obtained from Da Vinci Laboratory Solutions (The Netherlands). The aptamer used in this study was synthesised by Eurogentec (Belgium) with the following sequence: 5'-AGC-AGC-ACA-GAG-GTC-AGA-TGC-ACT-CGG-ACC-CCA-TTC-TCC-TTC-CAT-CCC-TCA-TCC-GTC-CAC-CCT-ATG-CGT-GCT-ACC-GTG-AA-3'. Aptamer solutions were prepared in Tris-buffer pH 7.4 from stock solutions. The water used in this study was ultrapure water (18.2 MΩ cm), purified in the laboratory (Milli-Q, Millipore, USA). All other chemicals used were of p.a. grade.

The multisine EIS set-up consisted of a Wenking POS 2 potentiostat (Bank Elektronik, Intelligent Controls GmbH, Germany) and a National Instruments PCI-4461 DAQ-card. The broadband multisine signal (see section 2.3) was digitally composed with Matlab software release 2014b (Mathworks Inc.). Matlab was also used to control the DAQ-card and the subsequent data processing.

The electrochemical measurements were performed in a conventional three-electrode cell configuration. The working electrode was a modified glassy carbon disk electrode (the aptasensor) and the auxiliary electrode was a platinum sheet electrode. A saturated Ag/AgCl electrode was used as reference electrode.

2.2. Fabrication of the sensing interface

The functionalized MWCNTs (MWCNT-COOH) were prepared as described in literature [39] by refluxing in a 3:1 sulphuric acid and nitric acid mixture. The functionalised MWCNTs were then dispersed in a 50:50 DMF and water mixture in a 0.5 mg/ml concentration.

The aptasensor was fabricated on a glassy carbon disk electrode (GCE). Prior to the modification, the electrode was mechanically polished with 1, 0.3 and 0.05 µm alumina slurry. Then 3 µl of the MWCNT-COOH suspension was uniformly dropped onto a polished GCE surface and the solvent was evaporated. The activation of the carboxylic acid groups of the MWCNTs was done by immersing the MWCNT/GCE in Tris-buffer containing 5 mM EDC and 8 mM NHS for 2 hours in a lightproof container. Subsequently the modified electrode was rinsed and then 8 µl of a 5 µM aptamer solution was dropped onto the surface for the covalent immobilization of the aptamer. The solution was left to incubate for 24 hours. The resulting aptasensor was rinsed with buffer prior to the measurements.

2.3. Multisine EIS signal

The excitation signal that was used in this work is an odd random phase multisine signal. This periodic broadband signal consists of the sum of harmonically related sine waves. Only the odd harmonics are excited and per group of 3 consecutive odd harmonics, one is randomly omitted. This creates multisine signal with a random harmonic grid which has a logarithmic distribution. An in-depth mathematical description can be found in [28] and [29].

The impedance measurements were performed at the open circuit potential of the system in the frequency range of 1 Hz - 20 kHz. Five consecutive periods of the excitation signal were measured and before processing, the first period was omitted to eliminate possible transients. The root-mean-square amplitude of the signal was set to 10 mV. All measurements were performed at room temperature in the buffer solution in presence of 10 mM $[Fe(CN)_6]^{3-/4-}$, used as a redox marker. The increment of R_{ct} is measured and calculated to a ratio to describe a quantitative model as follows:

$$\Delta R_{ct} = \frac{R_{ct_{Probe+OH-PCB}}}{R_{ct_{Probe}}} \quad (1)$$

To obtain the values of R_{ct}, the impedance spectra were plotted in Nyquist plots and a theoretical curve of the corresponding electrical equivalent circuit (EEC) was fitted to the spectra. A semicircle followed by a 45° straight line is described by the well-known Randles circuit [40,41]. However, the measured spectra show broadened semicircles, which can be described by the widely-used empirical model of the Randles circuit where the capacitor is replaced by a constant phase element. This is the circuit that was fitted to the data in this work (see figure 1 inset).

3. Results and discussion

3.1. Validation of the multisine impedimetric aptasensor

To validate the use of a broadband multisine signal for the aptasensor, a comparison is made to single sine. For this purpose the $[Fe(CN)_6]^{3-/4-}$ system is measured on a modified electrode (see 2.2) with both single sine and multisine as follows: a single sine EIS spectrum was measured and subsequently the cell was transferred to the multisine setup where a multisine EIS spectrum was measured. This experiment was done in triplicate.

The results of these measurements are shown in figure 1 and are in good agreement. The R_{ct} was determined to be (348 ± 22) Ω and (364 ±26) Ω for the single sine and multi sine measurements respectively. All other parameters and their errors were checked and no significant difference between the two techniques was found, in addition all errors were ≤3 % (and usually much lower) except for the CPE value which was ≤6%. It is clear that the multisine and single sine measurements yield similar results and that multisine EIS is suitable as signalling method for the aptasensor.

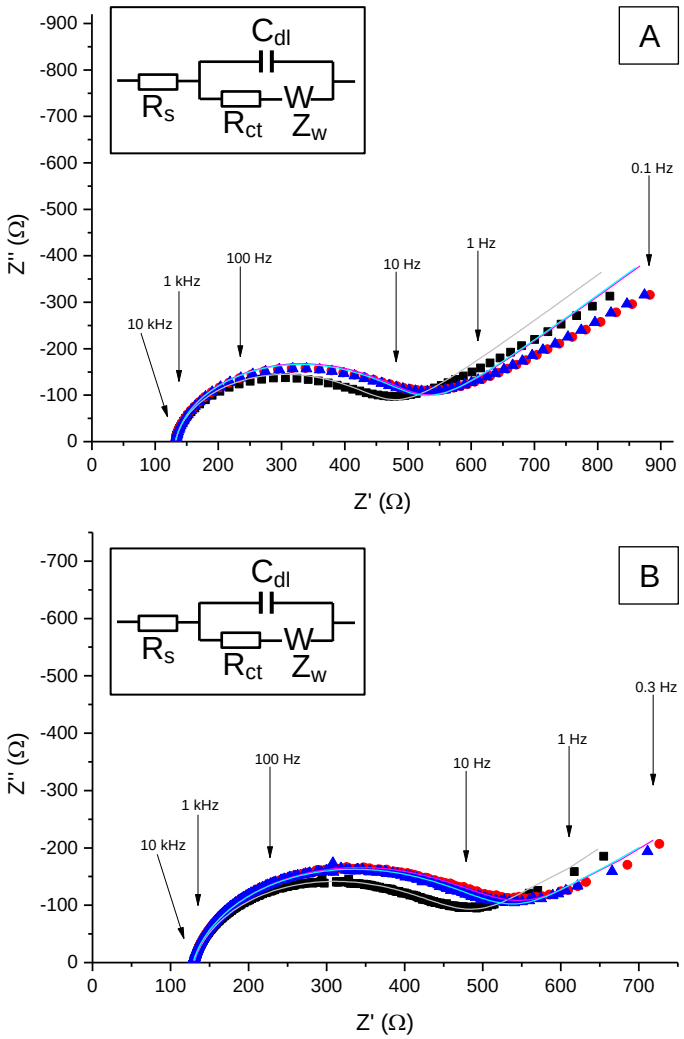

Figure 1: Comparison between consecutive single sine (a) and multisine (b) impedance measurements of the same aptasensor. The symbols represent the measured data and the solid lines the fitting results: black squares and grey line: measurement one, red dots and magenta line: measurement two, blue triangles and cyan line: measurement three.

3.2. Data analysis

ORP-EIS offers the possibility to determine the noise level and the contribution of non-linearities and non-stationarities at each frequency so that their influence can be taken into account when modelling the data. Figure 2 shows two measurements. The signal-to-noise ratio (SNR) can be calculated by comparing the amplitude of the impedance with the noise calculated from the non-excited frequencies. The linear behaviour of the system can be checked by comparing the total variance with the noise level at the non-excited

frequencies. If these curves do not coincide, the system under study shows non-linear behaviour. The stationarity of the system can be checked by comparing the noise at the excited frequencies with the noise at the non-excited frequencies. A difference between these two indicate non-stationair behaviour. More information can be found in [28,29].

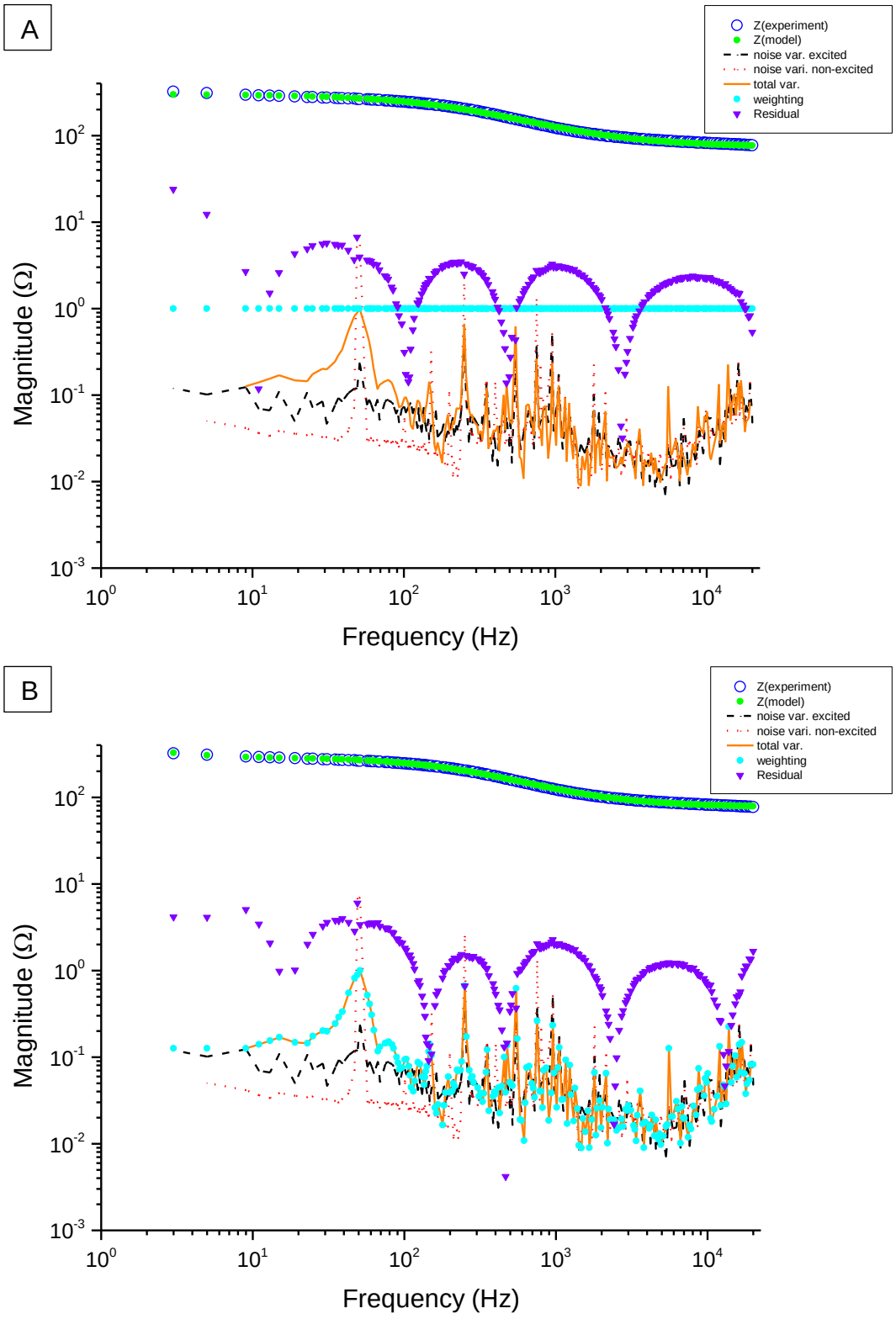

Figure 2: ORP-EIS measurement with fitting results of the aptasensor in presence of OH-PCB with unity

weighting (a) and total variance weighting (b). Measured impedance: blue circles, noise at excited frequencies: dashed black line, noise at non-excited frequencies: red plus signs, total variance (noise + non-linear distortions): solid yellow line, modelled impedance: green plus signs, weighting: cyan dots, residual curve (modelled - experimental): purple diamonds.

The possibility to check the quality of the experimental data allows the adaptation of the experimental conditions if necessary to minimize the contribution of the noise, the non-linearities and the non-stationarities. The remaining influences can then be taken into account when fitting the data. To obtain the best-fit values of the elements in the EEC, a cost function is minimized by means of a self-written procedure in matlab. The cost function f is defined as:

$$f(\theta) = \frac{1}{2}\sum_{i=1}^{N_{dp}} e_1^2 = \frac{1}{2}e^T e \tag{2}$$

Where N_{dp} is the number of datapoints and $e = e(\theta)$ the column vector (and e^T the transpose) with elements e_i which is the error between the experimental and simulated value for any value of θ the parameter vector in which all parameters of the EEC model are grouped. The fitting procedure estimates $\hat{\theta}$ – the value of θ which optimizes the correspondence between model and experiments – and minimizes f by a combination of the Gauss-Newton and Levenberg-Marquardt algorithms. Both involve the local evaluation of $f(\theta^{(k)})$ in a point $\theta^{(k)}$ based on a Taylor expansion of f limited to the quadratic term:

$$f\left(\bar{\theta}^{(k)} + \bar{\xi}\right) \approx f\left(\bar{\theta}^{(k)}\right) + \overline{\nabla} f(\bar{\theta}^{(k)})^T \bar{\xi} + \frac{1}{2}\bar{\xi}^T \overline{\nabla\nabla} f(\bar{\theta}^{(k)})\bar{\xi}$$

Where ∇ denotes the gradient operator, ξ the step size in the optimization process of the fitting and the super-script (k) refers to the iteration. For a more detailed explanation of the procedure the reader is referred to [42] and [43] where the underlying theory is explained and the procedure is applied to the $[Fe(CN)_6]^{3-/4-}$ redox couple.

In this fitting a weighting factor can be chosen to attach more weight to high-quality data points and less to low-quality data points. The weighting factor can be unity (all points equivalent weight), amplitude, noise level or total variance which includes the non-linearities. Using this weighting, it is possible to deduce the reliability of the parameters assessed from the fitting procedure, based on the experimental data.

As a case study, the aptasensor is measured in presence of OH-PCB. Figure 2 shows the result of fitting the data with unity weighting (figure 2 (a)) and total variance weighting (figure 2 (b)). In figure (a) the cyan dots form a straight line since unity weighting is chosen, in figure figure (b) the dots logically coincide with the total variance. The residual curve shows the difference between the modelled curve and the experimental data and is used to evaluate the model. In the ideal case that no measurement errors are present and that the model is correct, it should coincide with the measurement noise. However, in figure 2 there is a clear discrepancy of about an order of magnitude between the residual curve and the noise in both fittings. This means that the selected model does not represent the data properly. These results show that, although often proposed and used in literature, the Randles circuit might not be the best model to fit the data. Since it's not the scope of this

work, this part was not further elaborated, but the new sensing methodology clearly shows that improvement is possible.

3.3. Sensitivity and range

Measurements in presence of OH-PCB in a concentration range of (1 - 10) x 10^{-10} M were performed. Data analysis was performed as described in section 3.2 by fitting to a theoretical curve corresponding to the EEC with total variance weighting. The values of R_{ct} with the corresponding relative standard deviation (RSD) are tabulated in table 1. A ratio of ΔR_{ct} was calculated and a linear regression was performed. The resulting linear equation was $\Delta R_{ct} = 0.0214 C_{OH-PCB} + 1.10197$ with a Pearson's correlation coefficient of 0.971. The aptasensor shows good linear behaviour in the measured interval and OH-PCB could be detected in a concentration range of 10^{-10} M compared to the LOD of 10^{-8} for the amperometric aptasensor [19].

Table 1: Fitting values of R_{ct} and corresponding standard deviation, obtained by fitting with total variance weighting.

C_{OH-PCB} (10^{-10} M)	Value R_{ct} (Ω)	RSD (%)	Value ΔR_{ct}
0	178.0	0.55	1.000
2	188.9	0.48	1.061
4	201.8	0.47	1.134
6	207.8	0.45	1.167
8	208.8	0.44	1.174
10	218.3	0.36	1.226

4. Conclusions

In this work a multisine impedimetric aptasensing platform for OH-PCB is proposed. It is shown that by employing multisine instead of single sine, a number of advantages are obtained. Firstly by applying multiple sine signals at once, the shortest measurement time is obtained. This is a particularly relevant advantage for biosensors, where speeding up measurements is a challenging task. Secondly, by using an odd random phase multisine, the level of disturbing noise, the level of non-linear distortions and the level of non-stationary behaviour can be measured and quantified. This information can subsequently be incorporated in the fitting procedure by applying a weighting factor to the data, improving the accuracy and the reliability of the results. In addition, the model used for the fitting of the data can be checked. The aptasensor showed good linearity, reproducible results and was able to detect OH-PCB in a concentration range of 10^{-10} M. This is an improvement over the LOD of 10^{-8} for the earlier reported amperometric signalling method for the aptasensor. However, is it shown that the modelling might be erroneous and can be improved. The unique properties of the multisine EIS allow a thorough evaluation of the quality of the data and the model, leading to a fast, reliable and accurate electrochemical biosensing platform. This makes multisine not only a viable sensing option, but the preferable signalling technique.

References

[1] Y. Sapozhnikova, S.J. Lehotay, Multi-class, multi-residue analysis of pesticides, polychlorinated biphenyls, polycyclic aromatic hydrocarbons, polybrominated diphenyl ethers and novel flame retardants in fish using fast, low-pressure gas chromatography-tandem mass spectrometry, Anal.

Chim. Acta. 758 (2013) 80–92. doi:10.1016/j.aca.2012.10.034.

[2] G. Ottonello, A. Ferrari, E. Magi, Determination of polychlorinated biphenyls in fish: Optimisation and validation of a method based on accelerated solvent extraction and gas chromatography-mass spectrometry, Food Chem. 142 (2014) 327–333. doi:10.1016/j.foodchem.2013.07.048.

[3] T. Takasuga, K. Senthilkumar, K. Watanabe, Ultratrace analysis of polychlorinated biphenyls (PCBs) and their hydroxylated metabolites (OH-PCBs) in human serum and cerebrospinal fluid (CSF) samples, Organohalogen Compd. 66 (2004) 2501–2506.

[4] J. Mydlová-Memersheimerová, B. Tienpont, F. David, J. Krupčík, P. Sandra, Gas chromatography of 209 polychlorinated biphenyl congeners on an extremely efficient nonselective capillary column, J. Chromatogr. A. 1216 (2009) 6043–6062. doi:10.1016/j.chroma.2009.06.049.

[5] A. Posyniak, J. Zmudzki, J. Niedzielska, Evaluation of sample preparation for control of chloramphenicol residues in porcine tissues by enzyme-linked immunosorbent assay and liquid chromatography, Anal. Chim. Acta. 483 (2003) 307–311. doi:10.1016/S0003-2670(02)01487-3.

[6] C. Yang, B. Dou, K. Shi, Y. Chai, Y. Xiang, R. Yuan, Multiplexed and Ampli fi ed Electronic Sensor for the Detection of MicroRNAs from Cancer Cells, Anal. Chem. 86 (2014) 11913–11918. doi:10.1021/ac503860d.

[7] E. Silva, M. Mascini, S. Centi, A.P.F. Turner, Detection of Polychlorinated Biphenyls (PCBs) in Milk using a Disposable Immunomagnetic Electrochemical Sensor, Anal. Lett. 40 (2007) 1371–1385. doi:10.1080/00032710701327054.

[8] S.K. Yadav, B. Agrawal, P. Chandra, R.N. Goyal, In vitro chloramphenicol detection in a Haemophilus influenza model using an aptamer-polymer based electrochemical biosensor., Biosens. Bioelectron. 55 (2014) 337–42. doi:10.1016/j.bios.2013.12.031.

[9] D. Ueno, C. Darling, M. Alaee, L.M. Campbell, G. Pacepavicius, C. Teixeira, et al., Detection of hydroxylated polychlorinated biphenyls (OH-PCBs) in the abiotic environment: surface water and precipitation from Ontario, Canada., Environ. Sci. Technol. 41 (2007) 1841–1848. doi:10.1021/es061539l.

[10] V.M. Abraham, B.C. Lynn, Determination of hydroxylated polychlorinated biphenyls by ion trap gas chromatography – tandem mass spectrometry, J. Chromatogr. A. 790 (1997) 131–141.

[11] K. Nomiyama, S. Murata, T. Kunisue, T.K. Yamada, H. Mizukawa, S. Takahashi, et al., Polychlorinated biphenyls and their hydroxylated metabolites (OH-PCBs) in the blood of toothed and baleen whales stranded along Japanese coastal waters, Environ. Sci. Technol. 44 (2010) 3732–3738. doi:10.1021/es1003928.

[12] R.J. Letcher, H.X. Li, S.G. Chu, Determination of hydroxylated polychlorinated biphenyls (HO-PCBs) in blood plasma by high-performance liquid chromatography-electrospray ionization-tandem quadrupole mass spectrometry., J. Anal. Toxicol. 29 (2005) 209–216. doi:10.1093/jat/29.4.209.

[13] A.-E. Radi, J.L. Acero Sánchez, E. Baldrich, C.K. O'Sullivan, Reagentless, Reusable, Ultrasensitive Electrochemical Molecular Beacon Aptasensor, J. Am. Chem. Soc. 128 (2006) 117–124. doi:10.1021/ja053121d.

[14] T. Mairal, V. Cengiz Özalp, P. Lozano Sánchez, M. Mir, I. Katakis, C.K. O'Sullivan, Aptamers: molecular tools for analytical applications, Anal. Bioanal. Chem. 390 (2008) 989–1007. doi:10.1007/s00216-007-1346-4.

[15] A.-S. Cheng, K.R. Fleischmann, P. Wang, D.W. Oard, Advancing social science research by applying computational linguistics, Proc. Am. Soc. Inf. Sci. Technol. 45 (2009) 1–12.

doi:10.1002/meet.2008.1450450355.

[16] S. Pilehvar, J. Mehta, F. Dardenne, J. Robbens, R. Blust, K. De Wael, Aptasensing of Chloramphenicol in the Presence of Its Analogues: Reaching the Maximum Residue Limit, Anal. Chem. 84 (2012) 6753–6758. doi:10.1021/ac3012522.

[17] L. Yan, H. Guo, X. Sun, L. Shao, Q. Fang, Characterization of grass carp reovirus minor core protein VP4, Virol. J. 9 (2012). doi:10.1186/1743-422X-9-89.

[18] Z. Yan, N. Gan, D. Wang, Y. Cao, M. Chen, T. Li, et al., A "signal-on'' aptasensor for simultaneous detection of chloramphenicol and polychlorinated biphenyls using multi-metal ions encoded nanospherical brushes as tracers, Biosens. Bioelectron. 74 (2015) 718–724. doi:10.1016/j.bios.2015.07.024.

[19] S. Pilehvar, J. Ahmad Rather, F. Dardenne, J. Robbens, R. Blust, K. De Wael, Carbon nanotubes based electrochemical aptasensing platform for the detection of hydroxylated polychlorinated biphenyl in human blood serum, Biosens. Bioelectron. 54 (2014) 78–84. doi:10.1016/j.bios.2013.10.018.

[20] K. Turner, S. Xu, P. Pasini, S. Deo, L. Bachas, S. Daunert, Hydroxylated polychlorinated biphenyl detection based on a genetically engineered bioluminescent whole-cell sensing system, Anal Chem. 79 (2007) 5740–5745. doi:10.1021/ac0705162.

[21] S. Pilehvar, T. Dierckx, R. Blust, T. Breugelmans, K. De Wael, An Electrochemical Impedimetric Aptasensing Platform for Sensitive and Selective Detection of Small Molecules Such as Chloramphenicol, Sensors. 14 (2014) 12059–12069. doi:10.3390/s140712059.

[22] N. de-los-Santos-Álvarez, M.J. Lobo-Castañón, A.J. Miranda-Ordieres, P. Tuñón-Blanco, Aptamers as recognition elements for label-free analytical devices, TrAC - Trends Anal. Chem. 27 (2008) 437–446. doi:10.1016/j.trac.2008.03.003.

[23] E. Barsoukov, J.R. Macdonald, Impedance Spectroscopy Theory, Experiment, and Applications, 2nd ed., John Wiley & Sonc, Inc., 2005. doi:10.1002/0471716243.

[24] P. Agarwal, M.E. Orazem, L.H. Garcia-Rubio, Measurement Models for Electrochemical Impedance Spectroscopy I . Demonstration of Applicability, J. Electrochem. Soc. 139 (1992) 1917–1927. doi:10.1149/1.2069522.

[25] M.E. Orazem, P. Agarwal, C. Deslouis, B. Tribollet, Application of Measurement Models to Impedance Spectroscopy, J. Electrochem. Soc. 142 (1995) 948–960. doi:10.1149/1.2048479.

[26] W. Strunz, C. a. Schiller, J. Vogelsang, The evaluation of experimental dielectric data of barrier coatings in frequency- and time domain, Electrochim. Acta. 51 (2006) 1437–1442. doi:10.1016/j.electacta.2005.02.122.

[27] G.S. Popkirov, R.N. Schindler, Effect of sample nonlinearity on the performance of time domain electrochemical impedance spectroscopy, Electrochim. Acta. 40 (1995) 2511–2517. doi:http://dx.doi.org/10.1016/0013-4686(95)00075-P.

[28] E. Van Gheem, R. Pintelon, J. Vereecken, J. Schoukens, A. Hubin, P. Verboven, et al., Electrochemical impedance spectroscopy in the presence of non-linear distortions and non-stationary behaviour, Electrochim. Acta. 49 (2004) 4753–4762. doi:10.1016/j.electacta.2004.05.039.

[29] O.L. Blajiev, R. Pintelon, A. Hubin, Detection and evaluation of measurement noise and stochastic non-linear distortions in electrochemical impedance measurements by a model based on a broadband periodic excitation, J. Electroanal. Chem. 576 (2005) 65–72. doi:10.1016/j.jelechem.2004.09.029.

[30] Y. Van Ingelgem, E. Tourwé, O. Blajiev, R. Pintelon, A. Hubin, Advantages of odd random phase multisine electrochemical impedance measurements, Electroanalysis. 21 (2009) 730–739.

doi:10.1002/elan.200804471.

[31] T. Breugelmans, E. Tourwé, J.-B. Jorcin, A. Alvarez-Pampliega, B. Geboes, H. Terryn, et al., Odd random phase multisine EIS for organic coating analysis, Prog. Org. Coatings. 69 (2010) 215–218. doi:10.1016/j.porgcoat.2010.04.008.

[32] A. Alvarez-Pampliega, T. Hauffman, M. Petrova, T. Breugelmans, T. Muselle, K. Van Den Bergh, et al., Corrosion study on Al-rich metal-coated steel by odd random phase multisine electrochemical impedance spectroscopy, Electrochim. Acta. 124 (2014) 165–175. doi:10.1016/j.electacta.2013.09.159.

[33] A. Olsson, K. Ceder, Å. Bergman, B. Helander, Nestling Blood of the White-Tailed Sea Eagle (Haliaeetus albicilla) as an Indicator of Territorial Exposure to Organohalogen Compounds−An Evaluation, Environ. Sci. Technol. 34 (2000) 2733–2740. doi:10.1021/es991426k.

[34] T. Malmberg, J. Hoogstraate, A. Bergman, E. Klasson Wehler, Pharmacokinetics of two major hydroxylated polychlorinated biphenyl metabolites with specific retention in rat blood., Xenobiotica. 36 (2004) 581–589. doi:10.1080/00498250410001713078.

[35] T. Sinjari, P.O. Darnerud, H ydroxylated polychlorinated biphenyls : placental transfer and effects on thyroxine in the foetal mouse, Xenobiotica. 8 (1998) 21–30.

[36] A. Brouwer, K.J. van den Berg, Binding of a metabolite of 3,4,3',4'-tetrachlorobiphenyl to transthyretin reduces serum vitamin A transport by inhibiting the formation of the protein complex carrying both retinol and thyroxin., Toxicol. Appl. Pharmacol. 85 (1986) 301–312. doi:10.1016/0041-008X(86)90337-6.

[37] M.C. Lans, E. Klasson-Wehler, M. Willemsen, E. Meussen, S. Safe, A. Brouwer, Structure-dependent, competitive interaction of hydroxy-polychlorobiphenyls, -dibenzo-p-dioxins and -dibenzofurans with human transthyretin, Chem. Biol. Interact. 88 (1993) 7–21. doi:10.1016/0009-2797(93)90081-9.

[38] J.-Y. Park, S.-M. Park, DNA Hybridization Sensors Based on Electrochemical Impedance Spectroscopy as a Detection Tool, Sensors. 9 (2009) 9513–9532. doi:10.3390/s91209513.

[39] S. Niu, M. Zhao, L. Hu, S. Zhang, Carbon nanotube-enhanced DNA biosensor for DNA hybridization detection using rutin-Mn as electrochemical indicator, Sensors Actuators B Chem. 135 (2008) 200–205. doi:10.1016/j.snb.2008.08.022.

[40] M.E. Orazem, B. Tribollet, Electrochemical Impedance Spectroscopy, John Wiley & Sonc, Inc., 2008.

[41] A.J. Bard, L.R. Faulkner, Electrochemical methods: Fundamentals and Applications, 2nd ed., John Wiley & Sonc, Inc., 2001.

[42] E. Tourwé, R. Pintelon, A. Hubin, Extraction of a quantitative reaction mechanism from linear sweep voltammograms obtained on a rotating disk electrode. Part I: Theory and validation, J. Electroanal. Chem. 594 (2006) 50–58. doi:10.1016/j.jelechem.2006.05.028.

[43] E. Tourwé, T. Breugelmans, R. Pintelon, A. Hubin, Extraction of a quantitative reaction mechanism from linear sweep voltammograms obtained on a rotating disk electrode. Part II: Application to the redoxcouple, J. Electroanal. Chem. 609 (2007) 1–7. doi:10.1016/j.jelechem.2006.12.019.